Bioprocess and Biosystems Engineering (2020) 43:393–401
https://doi.org/10.1007/s00449-019-02235-1

RESEARCH PAPER

Electrochemical modeling of microbial fuel cells performance at different operating and structural conditions

Milad Kadivarian[2] · **Masoud Karamzadeh**[1]

Received: 5 July 2019 / Accepted: 16 October 2019 / Published online: 1 November 2019

Abstract

Organic matters are directly converted to electricity by microorganisms in microbial fuel cells (MFC). Modeling the performance of MFC sheds light on the behavior of MFC in various operational conditions (e.g. pH and temperature). In the present research, three voltage losses were considered for modeling of the MFC polarization curve. The current research is composed of two parts. In the first part, the polarization curves of various MFCs with different substrates (synthetic wastewater or industrial wastewaters) were reproduced by our model, and model parameters were obtained using experimental data and genetic algorithm optimization. In this part, the electrical performance of 26 systems (12 systems with synthetic wastewater and 14 systems with industrial wastewaters) were modeled with average relative error (ARE) of 17% and a coefficient of determination of 0.9. In the second part, the influence of temperature, pH and hydraulic retention time on the electrical performance of MFC were studied. In this part, parameters were estimated by conventional (estimation of model parameters in each point), and a novel method (estimation of model parameters as a function of operating parameters). It was shown that using second tuning method, the number of estimated parameters decreased, while the error of the model remained at an acceptable level.

Keywords Microbial fuel cell · Operating parameters · Structural parameters · Electrochemical model

List of symbols

A	Adjustable parameters of exchange current (Eq. 11–13)
ARE	Absolute relative error
b	Tafel's slope (V)
C	Concentration slope (V)
D	Adjustable parameters of limiting current (Eq. 11–13)
HRT	Hydraulic retention time (h)
i	Current (A)
OCV	Open circuit voltage (V)
R_{ohm}	Ohmic resistance (Ω)
R	Adjustable parameters of ohmic resistance (Eq. 11–13)
T	Temperature (K)
V	Voltage (V)
η	Potential (V)

Subscripts

act	Activation
an	Anode
cat	Cathode
ohm	Ohmic
l	Limiting
concen	Concentration
ex	Experiment
T	Temperature
h	HRT
p	PH

Introduction

Microbial fuel cells (MFC) are being considered for various applications, one of which is for the production of renewable energy. Direct conversion of harmful organic sources (e.g. industrial wastewater) to electricity is the most important advantage of MFC compared to other alternatives [1]. An MFC is an electrochemical bioreactor,

✉ Masoud Karamzadeh
m_karamzadeh@chemeng.iust.ac.ir

[1] Department of Chemical Engineering, Iran University of Science and Technology, Tehran, Iran

[2] Department of Chemical Engineering, Isfahan University of Technology, Isfahan, Iran

used to convert organic materials to electrons, protons and carbon dioxide by utilizing bacteria in the anode chamber. In a dual-chamber MFC, electrons are transferred to the anode by mediator, nanowire or direct mechanism. Then they are moved to the cathode via an external circuit. Protons are also transferred to the cathode by passing through the anolyte, a separating membrane, and the catholyte. In the cathode, electron acceptors (usually oxygen) receive electrons and protons producing water [2].

Zhang and Halm presented the first MFC model in 1995 [3]. Their model was used for simulation of the electrical performance of a dual-chamber MFC [3]. After this research, less attention was paid to MFC modeling for more than ten years. A new period of MFC modeling started in 2007 by introducing two–anode based models [4, 5]. MFC models are classified into two categories of comprehensive and specific models. The primary goal in comprehensive models is modeling the overall behavior of MFCs. These models are divided into two classes based on the limiting factor of the process. The first class of comprehensive models is known as anode and cathode based model, where the performance of an MFC is modeled by the anode and cathode reactions [6]. The second class of comprehensive type models is anode based models. The central assumption of anode based models is the assumption that the cathodic process (including reaction and mass transfer in the cathode chamber) are fast enough and the anodic process is the limiting factor of the MFC performance [4, 5, 7]. One of these two main models should be used for modeling the performance of MFC based on experimental and structural features. Therefore, in some cases [8-10] anode based models were the better choice for modeling (anodic process is the limiting factor). Also, in some cases, cathodic reaction must be considered [11-13].

Electrochemical model (polarization curve model) is one of the specific models [14, 15]. A practical and simple electrochemical model was introduced by Wen et al. [16]. Based on the electrochemical model, the polarization curve (voltage-current) can be divided into three regions: activation losses, ohmic losses, and concentration losses. The polarization curve model had seven adjustable parameters, which can be fitted on experimental data of a single-chamber continuous MFC with brewery wastewater as substrate [16].

Several researchers have focused on experimental evaluation of influence of structural parameters (electrode materials [17-19], and electrode modification [20]), operating parameters (temperature [21], hydraulic retention time (HRT) [22], and pH [23-25]) on performance of MFC.

However, modeling studies on the influence of these parameters on MFC performance are scarce. The details of MFC (e.g. source of voltage losses, the effect of operating variables such as temperature and pH) can be understood by electrochemical modeling results. That means electrochemical results help researchers to improve MFC performance by creating MFCs with lower voltage losses.

In the present research, a two-part-specific modeling (polarization curve modeling) for the electrical behavior of MFC was carried out by using genetic algorithm optimization method. In the first part, model parameters of MFC with different substrates were validated against experimental data, and the polarization curve was reproduced by the model. The effect of operating and structural parameters on source of voltage losses cannot be directly investigated by electrochemical modeling. However, in the second part of present research, a simple procedure was suggested and examined for studying the effect of structural and operating parameters on the electrical performance of MFC. To investigate the effect of operating parameters such as temperature, hydraulic retention time and pH, on the electrical performance of MFC, a novel method for estimation of parameters was used by defining model parameters as functions of operating conditions.

Model development

The polarization curve of fuel cells contains three regions: activation, ohmic, and concentration regions. The energy required to overcome the activation barrier of anodic and cathodic reactions is represented by activation loss. Activation loss decreases by modifying the cathode catalyst. Resistances against ions transfer in catholyte, anolyte, separator, and electrodes were defined as ohmic losses. Ohmic losses decrease with increasing conductivity of electrolytes. Limitation of chemical species which were transported in chambers (anode and cathode chamber), considered as concentration loss [16, 26]. The voltage of MFC was defined as follows:

$$V = \mathrm{OCV} - \eta_{\mathrm{act}} - \eta_{\mathrm{ohm}} - \eta_{\mathrm{concen}}, \tag{1}$$

where, OCV, η_{act}, η_{ohm} and η_{concen} were open-circuit voltage (V) (voltage in no current), activation loss (V), ohmic loss (V) and concentration loss (V), respectively. Activation loss was divided into anode and cathode activation losses. Voltage activation losses were defined by Tafel's equation (Eqs. 3–4).

$$\eta_{\mathrm{act}} = \eta_{\mathrm{ca}} + \eta_{\mathrm{an}}, \tag{2}$$

$$\eta_{\mathrm{an}} = b_{\mathrm{an}} \times \ln\left(\frac{i}{i_0}\right), \tag{3}$$

$$\eta_{\mathrm{ca}} = b_{\mathrm{ca}} \times \ln\left(\frac{i}{i_0}\right), \tag{4}$$

where, b_{an}, b_{ca}, i_0 and i represent Tafel's slope of the anode (V), cathode (V), exchange current (A) and current (A), respectively. Activation loss (Eqs. 5 and 6) obtained with substituting Eqs. 3 and 4 in Eq. 2.

Table 1 Model parameters of MFC with synthetic wastewater as a carbon source

Feed	Type of MFC	i_0 (A)	b (V)	R_{ohm} (Ω)	C (V)	i_l (A)	ARE%	R^2	Ref.1
Cellulose	DC[2]	$1.38*10^{-5}$	0.033	315.46	0.398	0.0016	4.45	0.998	[37]
Sucrose[3,*]	SC[4]	$9.48*10^{-6}$	$1*10^{-4}$	687.3	0.0788	0.0011	4.57	0.992	[27]
**	SC	$1.22*10^{-5}$	0.047	150.9	0.102	0.0030	3.69	0.99	[27]
***	SC	$3.59*10^{-5}$	0.018	103.5	0.016	0.0096	4.11	0.995	[27]
Sucrose	DC	$7.92*10^{-4}$	0.015	3.242	0.114	0.170	5.6	0.992	[38]
Fructose	DC	$7.91*10^{-4}$	0.011	3.299	0.105	0.19	7.11	0.991	[38]
Glucose	DC	$8.0*10^{-4}$	0.009	3.28	0.08	0.199	6.89	0.997	[38]
Xylose	DC	$4.6*10^{-3}$	0.001	96.8	0.102	0.007	5.54	0.986	[39]
Acetate	SC	$7.02*10^{-5}$	0.01	0.038	0.074	34.34	5.26	0.979	[40]
Glycerol	SC	$1.21*10^{-5}$	0.08	8.54	0.018	0.86	7.15	0.87	[41]
Ethanol	DC	$1.27*10^{-6}$	0.018	946	0.107	0.0013	8.68	0.975	[42]
Ethanol	SC	$3.46*10^{-6}$	0.028	131.4	0.035	0.0014	2.4	0.985	[42]

[1]Reference of experimental data

[2]Dual-chamber MFC

[3]MFC with same substrate and different anode electrode materials (*graphite rod, **triangles of graphite, ***graphite flakes)

[4]Single-chamber MFC

$$\eta_{act} = b_{ca} \times \ln\left(\frac{i}{i_0}\right) + b_{an} \times \ln\left(\frac{i}{i_0}\right), \quad (5)$$

$$\eta_{act} = b_{act} \times \ln\left(\frac{i}{i_0}\right), \quad (6)$$

The Ohmic loss was represented by Eq. 7 [16].

$$\eta_{ohm} = R_{ohmic} i. \quad (7)$$

Based on Eq. 7, the ohmic resistances in MFC are shown by R_{ohmic} (Ω). The concentration loss was introduced as in Eq. 3 [16]:

$$\eta_{concen} = C \times \ln\left(\frac{i_l}{i_l - i}\right). \quad (8)$$

In Eq. 8, C and i_l are concentration loss slope (V) and limiting current (A). Limiting current is the maximum producible current in MFC. The general polarization equation was obtained by substituting Eqs. 6 and 7 and 8 into Eq. 1.

$$V = OCV - \left(b \times \ln\left(\frac{i}{i_0}\right)\right) - (R_{ohmic} i) - \left(C \times \ln\left(\frac{i_l}{i_l - i}\right)\right). \quad (9)$$

Equation 9, was the final equation utilized for modeling of polarization curve. This equation has five unknown parameters (B, i_0, R_{ohmic}, C, and i_l). These parameters were fitted on experimental data of voltage-current by using the optimization algorithm. Optimization algorithm adjusted unknown parameters by minimizing the objective function. In the present research, relative squared error (RSE) (Eq. 19) was used as an objective function for parameters estimation.

$$RSE = \sum \sqrt{\left(\frac{V_{Model} - V_{Ex}}{V_{Ex}}\right)^2}. \quad (10)$$

Modeling of the polarization curve was carried out by MATLAB software. Search domain of parameter estimation was limited to an acceptable range. Genetic algorithm with a population of 1,000,000 individuals, elite count of 5% and a crossover of 0.8 was used for adjusting unknown parameters. The accuracy of model output was shown by absolute relative error (ARE %) and the coefficient (R^2).

Results and discussion

The polarization curve model has five unknown parameters with different effects on voltage overpotential. Voltage losses decreased with an increase in exchange and limiting

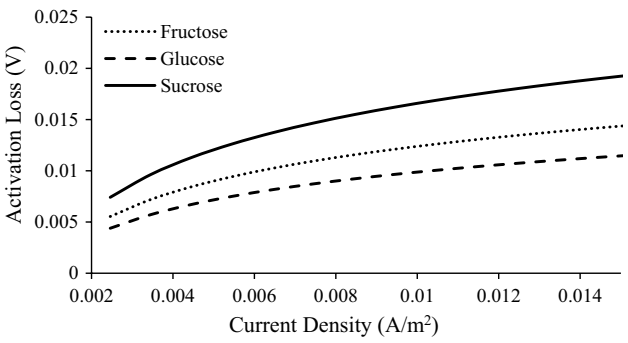

Fig. 1 Activation loss of MFC with carbohydrate as substrate

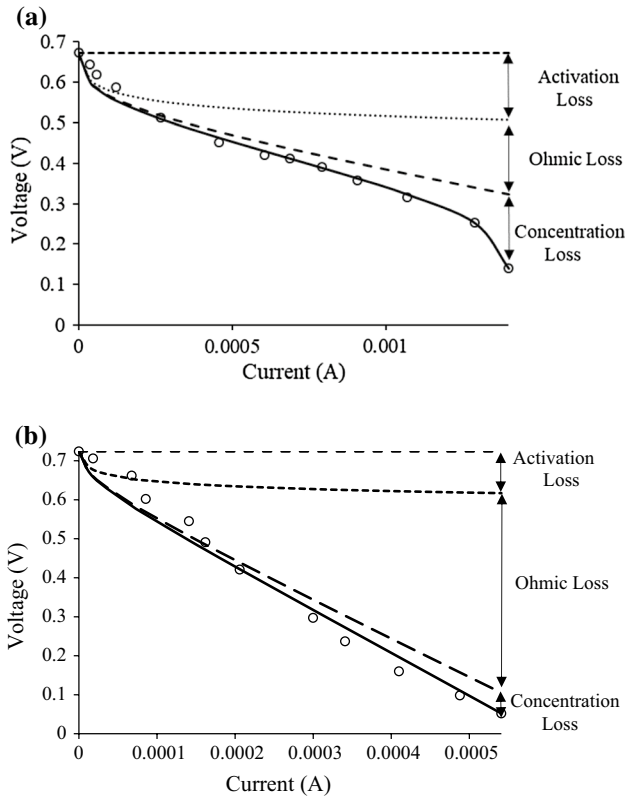

Fig. 2 Results of polarization curve modeling of **a** single-chamber, **b** dual-chamber MFC with ethanol as substrate (o) experimental point (solid line) model output

current. However, increasing Tafel's slope, ohmic resistance and concentration loss slope led to increasing voltage losses. Modeling the electrical performance of MFC was carried out in two parts:

- Investigation of the influence of various substrate
- Investigation of the effect of operating parameters on the performance of MFC.

MFC with various substrates

The polarization curve of MFC was modeled by two different types of substrates. The results of estimated parameters of 11 systems with synthetic wastewater are presented in Table 1. References of experimental data, used for validating the model are presented in the last column of Table 1. The results show that ARE < 9% and the coefficient of determination (R^2) > 0.87. Therefore, the results are in good agreement between model output and experimental data. Also, modeling behavior of MFC with different anode materials (Graphite rod, Triangles of graphite and Graphite flakes) were studied and the results are shown in Table 1. Based on experimental results, the higher surface area of anode [27] or higher surface contact between microorganisms and anode [28] leads to higher produced power. The results show that the concentration loss was responsible for most of voltage loss in MFC with a graphite rod. However, in other two anode materials, the major part of voltage loss was due to ohmic losses. Comparing the concentration losses in MFC with three anode materials, indicated that

Table 2 Model parameters of MFC with industrial wastewater as a carbon source

Wastewater	MFC	i_0 (A)	b (V)	R_{ohm} (Ω)	C (V)	i_l (A)	ARE%	R^2	Ref
Brewery[1]	DC	$4.98*10^{-7}$	0.053	10	0.012	0.021	3.51	0.991	[43]
2	DC	$8.24*10^{-6}$	0.089	1.1	0.047	0.026	4.5	0.973	[43]
Biodiesel	SC	$5.41*10^{-5}$	0.014	267.3	0.07	0.002	8.46	0.974	[44]
Petroleum	SC	0.038	$1*10^{-5}$	0.08	0.186	3.243	2.24	0.996	[45]
Urine	SC	$2.51*10^{-5}$	0.094	240	0.009	0.00059	3.58	0.993	[46]
Distillery	SC	0.045	0.094	6.1	0.0123	6	4.41	0.995	[36]
Urban[3]	SC	$6.56*10^{-5}$	0.039	84.8	0.008	0.015	10.3	0.995	[47]
4	SC	$1.55*10^{-5}$	0.067	124.9	0.036	0.015	14.25	0.943	[47]
Brewery	SC	$3.26*10^{-5}$	0.045	21.2	0.064	0.007	3.05	0.997	[16]
Seafood	DC	$2.01*10^{-5}$	0.015	96.2	0.014	0.096	7.34	0.982	[35]
Dairy	SC	$3.4*10^{-10}$	0.007	61.6	0.324	0.005	7.04	0.972	[48]
Cashew apple juice	DC	$7.07*10^{-6}$	0.04	74.9	0.041	0.016	4.3	0.995	[49]
Chemical	DC	$1.53*10^{-7}$	0.017	63.4	0.03	0.01	7.98	0.91	[23]
Rice straw	DC	$2.14*10^{-4}$	0.002	60.5	0.87	0.006	3.98	0.987	[50]
Milk industry	DC	$8.98*10^{-6}$	0.039	170.6	0.06	$9.10*10^{-4}$	6.06	0.96	[10]
Soya industry	DC	$1.10*10^{-7}$	0.039	130.0	0.049	$5.65*10^{-4}$	10.3	0.96	[10]
Cocking food		$2.16*10^{-5}$	0.004	250.1	0.112	0.006	4.02	0.99	[51]

[1]pH = 7, [2]pH = 10, [3]pH = 9.5, [4]pH = 7.5

concentration loss in MFC with graphite rod anode was higher than the other two materials. As mentioned above, concentration loss of voltage was due to the mass transfer limitations of chemical species into or out of anode. Rate of mass transfer depends on the surface area of anode. The surface areas for graphite rod, triangles of graphite, and graphite flakes were 0.000889, 0.062 and 0.28 m^2, respectively. Therefore, concentration loss in MFC with graphite rod was higher than triangles of graphite and graphite flakes [27] due to its higher surface area. According to Table 1, the results show that ohmic resistance of MFC with graphite rod anode electrode was higher than the other MFCs ($R_{\text{ohm., graphite rod}} > R_{\text{ohm., triangles of graphite}} > R_{\text{ohm., graphite flakes}}$). This result is in accordance with previous experimental results [27]. Nevertheless, MFC with triangles of graphite showed the highest activation loss.

Polarization curve of dual-chamber MFC with various carbohydrates (fructose, glucose, and sucrose with a concentration of 20 g/L) as substrates was modeled and results are presented in rows 5–7 of Table 1. Based on the modeling results, ohmic resistances of MFC remained approximately the same for various substrates. Activation losses in MFC with various carbohydrates as substrates are presented in Fig. 1. Based on Fig. 1, activation loss in MFC with monosaccharides was lower than disaccharides. This was attributed to the different mechanisms in converting disaccharides (sucrose) and monosaccharides (glucose and fructose) to electricity. Concentration loss was small when the mass transfer of chemical species in or from anode was fast. In the same bulk concentration of substrate, higher diffusion coefficient can lead to higher rates of mass transfer to anode [29]. Therefore, concentration loss in MFC with disaccharides (sucrose) was higher than monosaccharides (glucose and fructose).

Experimental and reproduced polarization curve of single- and dual-chamber MFC with ethanol substrate are shown in Fig. 2a, b. The results indicate that ohmic resistance of single-chamber MFC was lower than dual-chamber type. Dual-chamber MFC had two sources of ohmic resistance (separator and catholyte) more than single-chamber MFC. This fact may be the reason for higher ohmic resistance in dual-chamber MFC. According to Fig. 2b major part

Table 3 Modeling results at different operating conditions

Substrate		i_0 (A)	b (V)	R_{ohm} (Ω)	C (V)	i_1 (A)	ARE%	R^2	Ref
	Temperature (K)								
Glucose	299	$4.95*10^{-6}$	0.049	996.8	0.097	$3.84*10^{-4}$	6.37	0.983	[52]
	303	$1.65*10^{-5}$	0.05	899.0	0.116	$5.19*10^{-4}$	4.85	0.995	[52]
	306	$2.30*10^{-5}$	0.069	799.9	0.136	$6.65*10^{-4}$	2.33	0.996	[52]
	308	$3.79*10^{-5}$	0.076	698.6	0.148	$8.51*10^{-4}$	2.28	0.996	[52]
Acetate	277	$8.77*10^{-7}$	0.035	205.9	0.079	0.0097	3.06	0.993	[53]
	283	$1.77*10^{-5}$	0.063	168.6	0.149	0.0098	5.74	0.988	[53]
	288	$4.82*10^{-5}$	0.063	140.2	0.150	0.0119	4.55	0.982	[53]
	293	$1.19*10^{-4}$	0.063	110	0.150	0.0129	9.93	0.961	[53]
	303	$1.19*10^{-4}$	0.069	70	0.151	0.015	13.46	0.95	[53]
	HRT (h)								
Glucose	16	$1.44*10^{-5}$	0.036	284.1	0.124	0.009	1.9	0.996	[34]
	12.33	$2.31*10^{-5}$	0.038	237.3	0.043	0.010	3.29	0.993	[34]
	6.33	$2.38*10^{-5}$	0.062	182.1	0.104	0.015	2.39	0.994	[34]
	3.6	$2.24*10^{-5}$	0.047	272.2	0.143	0.012	2.05	0.997	[34]
Cafeteria	6	$7.47*10^{-4}$	0.0001	22.0	0.018	0.012	10.7	0.922	[22]
Wastewater	4	$8.55*10^{-4}$	0.00004	20.6	0.057	0.017	8.25	0.952	[22]
	2	$1.00*10^{-3}$	0.00002	15.0	0.176	0.022	7.63	0.962	[22]
	1	$1.6*10^{-3}$	0.00003	10.0	0.217	0.035	7.66	0.974	[22]
	pH								
Lactate1	5	$8.95*10^{-8}$	0.035	2541.0	0.458	0.008	4.2	0.995	[33]
	6	$1.19*10^{-7}$	0.056	192.3	0.022	0.011	3.79	0.997	[33]
	7	$2.62*10^{-7}$	0.051	199.9	0.499	0.01	8.43	0.996	[33]
	5	$8.92*10^{-8}$	0.052	143.2	0.266	0.002	3.61	0.998	[33]
	6	$1.18*10^{-7}$	0.059	101.1	0.469	0.005	6.36	0.99	[33]
	7	$7.57*10^{-8}$	0.046	165.6	0.707	0.004	4.33	0.998	[33]

[1]MFC with two different microorganisms, rows 18–20 Shewanella oneidensis DSP10 and rows 21–23 Shewanella oneidensis MR-1

of voltage loss was due to ohmic resistances in dual-chamber MFC.

Results of polarization curve modeling of 14 MFC systems with industrial wastewater as substrate are presented in Table 2. These systems were selected from different types of wastewater, reported in literature [30, 31]. In order to be able to reproduce some of the results, in these systems the open-circuit voltage must be reported. Comparing reproduced polarization curve and experimental data indicated acceptable accuracy of the model ($R^2 > 0.91$ and ARE < 15%).

Modeling effect of temperature, pH and HRT on the performance of MFC

The effects of operating parameters (temperature, HRT and pH) on electrical performance were modeled and results are reported in Table 3. MFCs with glucose at temperature 299–308 K and acetate at 277–303 K (Table 3 rows 1–8) were modeled. Ohmic resistance decreased with increasing temperature. However, other parameters (Tafel's slope, exchange current, concentration loss slope and limiting current) increased when temperature was increased.

It was shown that increasing temperature would lead to decreasing ohmic resistance. This was due to the fact that anolyte resistance against ion transport decreased by increasing temperature. Limiting current depends on diffusion coefficient [29] and diffusion coefficient increases with increasing temperature [32]. Therefore, limiting current increased with increasing temperature. The estimated value of ohmic resistance, exchange and limiting current at different temperatures are reported in Fig. 3. According to Fig. 3 and Table 3 (rows 1–8 and columns 2–7), estimated parameters have linear relation with temperature.

As a novel method, the model parameters were fitted on a temperature-dependent relation. This relation was obtained based on modeling results and is shown in Eq. 11. Also, the performance of this relation was examined. Reducing the number of fitting parameters of MFC with glucose from 20 to 6 and MFC with acetate from 25 to 6 adjustable parameters was one of the most important advantages of the new method of parameter estimation.

$$i_0 = A_T T,\ b = B_T T,\ R_{\text{ohm}} = R_{1T} T + R_{2T},\ C = C_T T,\quad i_l = D_T T, \tag{11}$$

where, A_T, B_T, R_{1T}, R_{2T}, C_T, and D_T were six adjustable parameters, fitted on experimental data at different temperatures. New model Parameters (six unknown parameters of Eq. 11) were estimated and reported in Table 4. Model error was defined as the difference between reproduced polarization curve by model and experimental data. This error remained at an acceptable level, while adjustable parameters decreased significantly.

Effects of HRT and pH on performance of MFC were more complicated, compared to temperature. There is an optimum value of these parameters, where MFC shows its optimum performance [22, 33, 34]. Based on the results presented in Table 3, exchange and limiting current show a maximum, while ohmic resistance shows a minimum. So Second-order relations (Eqs. 12 and 13) were suggested for modeling the effect of HRT and pH.

$$\begin{aligned} i_0 &= A_{1h}\text{HRT}^2 + A_{2h}\text{HRT} + A_{3h} \\ R_{\text{ohm}} &= R_{1h}\text{HRT}^2 + R_{2h}\text{HRT} + R_{3h}\,, \\ i_l &= D_{1h}\text{HRT}^2 + D_{2h}\text{HRT} + D_{3h} \end{aligned} \tag{12}$$

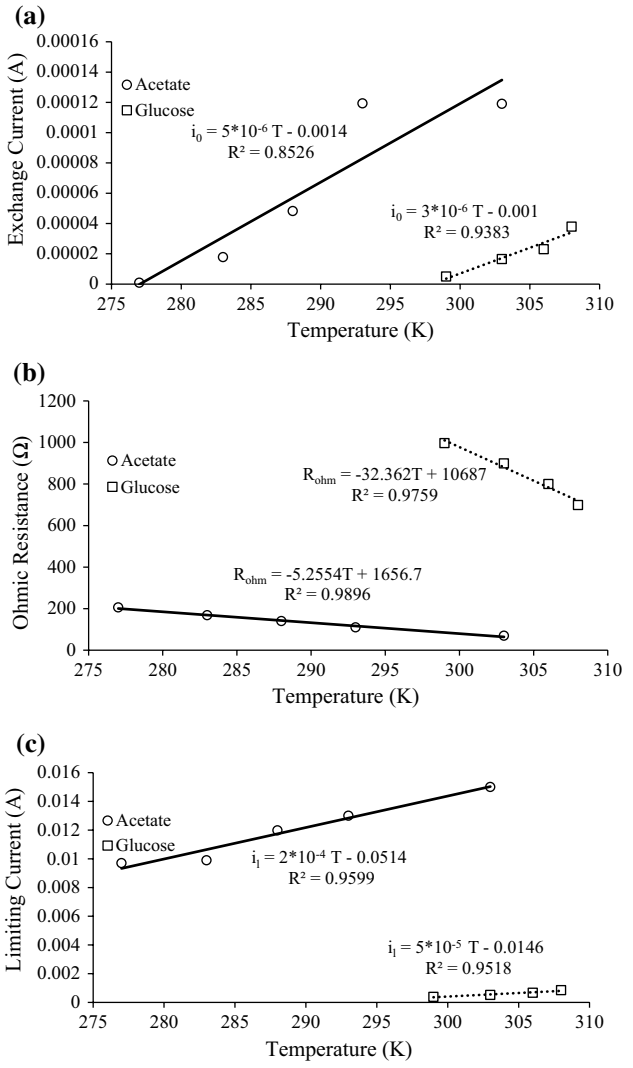

Fig. 3 Model parameters (**a** exchange current, **b** ohmic resistance and **c** limiting current) at different temperature based on results reported in Table 3

Table 4 Estimated parameters of Eq. 11

Substrate	Tem. (K)	A_T	B_T	R_{2T}	R_{1T}	C_T	D_T	ARE%	R^2
Glucose	299–308	$3.09*10^{-9}$	$2.63*10^{-5}$	27,105.1	-83.9	$54.54*10^{-4}$	$5.183*10^{-4}$	10.36	0.994
Acetate	277–303	$2.16*10^{-16}$	$3.28*10^{-5}$	1812.4	-5.73	$1.12*10^{-4}$	$3.14*10^{-4}$	10.7	0.994

Table 5 Estimated parameters of Eqs. 12 and 13

HRT			pH		
Substrate	Glucose	Domestic	Substrate	Lactate	Lactate
HRT range (h)	3.6–16	1–6	pH range	5–7	5–7
A_{1h}	$-1.00*10^{-11}$	0.0789	A_{1h}	$1.934*10^{-8}$	$1.7*10^{-8}$
A_{2h}	$2.38*10^{-5}$	− 0.0029	A_{2h}	$-8.43*10^{-8}$	$-1.6*10^{-7}$
A_{3h}	$1.15*10^{-5}$	0.0031	A_{3h}	$5.8*10^{-7}$	$4.7*10^{-7}$
B	0.0461	0.0224	B	0.07	0.055
R_{1h}	649.8	− 140.92	R_{1h}	$-9.58*10^{-22}$	$-7.11*10^{-13}$
R_{2h}	− 474.62	106.11	R_{2h}	1.39	0.255
R_{3h}	301.20	1.0782	R_{3h}	94.65	99.27
C	0.494	0.261	C	0.064	0.12
D_{1h}	− 0.197	1.2084	D_{1h}	$5.05*10^{-4}$	$4.88*10^{-4}$
D_{2h}	0.1696	− 0.28777	D_{2h}	$-4.1*10^{-3}$	− 0.06
D_{3h}	0.0121	0.044	D_{3h}	0.078	0.019
ARE%	3.74	15.17	ARE%	11.3	9.14
R^2	0.991	0.961	R^2	0.966	0.979

$$\begin{aligned} i_0 &= A_{1p}\mathrm{pH}^2 + A_{2p}\mathrm{pH} + A_{3p} \\ R_{\mathrm{ohm}} &= R_{1p}\mathrm{pH}^2 + R_{2p}\mathrm{pH} + R_{3p}, \\ i_l &= D_{1p}\mathrm{pH}^2 + D_{2p}\mathrm{pH} + D_{3p} \end{aligned} \tag{13}$$

where A_{ih}, A_{ip}, R_{ih}, R_{ip} and D_{ih}, D_{ip} ($i = 1$, 2 and 3) were adjustable parameters, fitted on experimental data at different HRT and pH. There are eleven unknown parameters, which must be fitted on polarization curve data at different operating conditions (HRT and pH). In order to use Eqs. 12 and 13, the polarization curve must be known in at least three pH or HRT values. Equations 11–13 can be used for reproducing polarization curve of MFC in each point between the minimum and maximum value of operating parameters (temperature, HRT and pH). This is advantageous compared to the usual methods, where estimated parameters are limited to conditions of their adjustment (Table 5).

Results of the new method of parameter estimation in terms of temperature show that the average number of adjustable parameters decreased by more than 70%, while R^2 remained higher than 95%. For HRT and pH, the number of unknown parameters decreased more than 45 and 25% while, ARE increased by about 4 and 5%, respectively. It should be noted that operating conditions changed during electricity production by MFC [35, 36]. Also, the new method can be used between the minimum and maximum value of operating parameters with an acceptable level of error. Finally, it was shown that Eqs. 11–13 were suitable in modeling the practical application of MFC in real conditions.

Conclusion

In the present research, the polarization curve model was used for simulation of the electrical performance of an MFC at different conditions. In the first part of the current study, the electrical performance of MFC was modeled for two different types of substrates. Polarization curves of 12 synthetic and 14 industrial wastewater systems were modeled with $R^2 > 0.87$ and $R^2 > 0.91$, respectively. Moreover, the effects of anode materials and type of MFC (single- or dual-chambers) on the electrical behavior of MFC were modeled. The results showed that ohmic resistance in dual-chamber MFC was higher than single-chamber type. In the second part, the effect of three operating parameters (temperature, HRT and pH) on the performance of MFC was simulated with two different methods of parameter estimation. A new method of parameter estimation was proposed and the results showed that the model error remained at an acceptable level ($R^2 > 0.95$), while the number of adjustable parameters decreased significantly.

Compliance with ethical standards

Conflict of interest The authors declare that they have no known competing financial interests or personal relationships that could have appeared to influence the work reported in this paper.

References

1. Guo X, Zhan Y, Chen C, Cai B, Wang Y, Guo S (2016) Influence of packing material characteristics on the performance of microbial fuel cells using petroleum refinery wastewater as fuel. Renew Energy 87:437–444. https://doi.org/10.1016/j.renene.2015.10.041
2. Logan BE (2007) Introduction. In: Microbial fuel cells. Wiley, USA, pp 1–11. doi:10.1002/9780470258590.ch1.
3. Zhang X-C, Halme A (1995) Modelling of a microbial fuel cell process. Biotechnol Lett 17(8):809–814. https://doi.org/10.1007/BF00129009
4. Kato Marcus A, Torres CI, Rittmann BE (2007) Conduction-based modeling of the biofilm anode of a microbial fuel cell. Biotechnol Bioeng 98(6):1171–1182. https://doi.org/10.1002/bit.21533
5. Picioreanu C, Head IM, Katuri KP, van Loosdrecht MCM, Scott K (2007) A computational model for biofilm-based microbial fuel cells. Water Res 41(13):2921–2940. https://doi.org/10.1016/j.watres.2007.04.009
6. Zeng Y, Choo YF, Kim B-H, Wu P (2010) Modelling and simulation of two-chamber microbial fuel cell. J Power Sources 195(1):79–89. https://doi.org/10.1016/j.jpowsour.2009.06.101
7. Picioreanu C, van Loosdrecht MCM, Curtis TP, Scott K (2010) Model based evaluation of the effect of pH and electrode geometry on microbial fuel cell performance. Bioelectrochemistry 78(1):8–24. https://doi.org/10.1016/j.bioelechem.2009.04.009
8. Mahdi Mardanpour M, Nasr Esfahany M, Behzad T, Sedaqatvand R (2012) Single chamber microbial fuel cell with spiral anode for dairy wastewater treatment. Biosens Bioelectron 38(1):264–269. https://doi.org/10.1016/j.bios.2012.05.046
9. Jayasinghe N, Franks A, Nevin KP, Mahadevan R (2014) Metabolic modeling of spatial heterogeneity of biofilms in microbial fuel cells reveals substrate limitations in electrical current generation. Biotechnol J 9(10):1350–1361. https://doi.org/10.1002/biot.201400068
10. Pant D, Van Bogaert G, Álvarez-Gallego Y, Diels L, Vanbroekhoven K (2016) Evaluation of bioelectrogenic potential of four industrial effluents as substrate for low cost microbial fuel cells operation. Environ Eng Manag J 15(8):1897–1904
11. Rossi R, Jones D, Myung J, Zikmund E, Yang W, Gallego YA, Pant D, Evans PJ, Page MA, Cropek DM, Logan BE (2019) Evaluating a multi-panel air cathode through electrochemical and biotic tests. Water Res 148:51–59. https://doi.org/10.1016/j.watres.2018.10.022
12. Mashkour M, Rahimnejad M, Pourali SM, Ezoji H, ElMekawy A, Pant D (2017) Catalytic performance of nano-hybrid graphene and titanium dioxide modified cathodes fabricated with facile and green technique in microbial fuel cell. Prog Nat Sci Mater Int 27(6):647–651. https://doi.org/10.1016/j.pnsc.2017.11.003
13. Pasupuleti SB, Srikanth S, Dominguez-Benetton X, Mohan SV, Pant D (2016) Dual gas diffusion cathode design for microbial fuel cell (MFC): optimizing the suitable mode of operation in terms of bioelectrochemical and bioelectro-kinetic evaluation. J Chem Technol Biotechnol 91(3):624–639. https://doi.org/10.1002/jctb.4613
14. Ortiz-Martínez VM, Salar-García MJ, de los Ríos AP, Hernández-Fernández FJ, Egea JA, Lozano LJ (2015) Developments in microbial fuel cell modeling. Chem Eng J 271:50–60. https://doi.org/10.1016/j.cej.2015.02.076
15. Harnisch F, Warmbier R, Schneider R, Schröder U (2009) Modeling the ion transfer and polarization of ion exchange membranes in bioelectrochemical systems. Bioelectrochemistry 75(2):136–141. https://doi.org/10.1016/j.bioelechem.2009.03.001
16. Wen Q, Wu Y, Cao D, Zhao L, Sun Q (2009) Electricity generation and modeling of microbial fuel cell from continuous beer brewery wastewater. Bioresour Technol 100(18):4171–4175. https://doi.org/10.1016/j.biortech.2009.02.058
17. Özkaya B, Cetinkaya AY, Cakmakci M, Karadağ D, Sahinkaya E (2013) Electricity generation from young landfill leachate in a microbial fuel cell with a new electrode material. Bioprocess Biosyst Eng 36(4):399–405. https://doi.org/10.1007/s00449-012-0796-z
18. Kakarla R, Min B (2014) Evaluation of microbial fuel cell operation using algae as an oxygen supplier: carbon paper cathode vs carbon brush cathode. Bioprocess Biosyst Eng 37(12):2453–2461. https://doi.org/10.1007/s00449-014-1223-4
19. Ozkaya B, Akoglu B, Karadag D, Acı G, Taskan E, Hasar H (2012) Bioelectricity production using a new electrode in a microbial fuel cell. Bioprocess Biosyst Eng 35(7):1219–1227. https://doi.org/10.1007/s00449-012-0709-1
20. Nourbakhsh F, Mohsennia M, Pazouki M (2017) Nickel oxide/carbon nanotube/polyaniline nanocomposite as bifunctional anode catalyst for high-performance Shewanella-based dual-chamber microbial fuel cell. Bioprocess Biosyst Eng 40(11):1669–1677. https://doi.org/10.1007/s00449-017-1822-y
21. Heidrich ES, Dolfing J, Wade MJ, Sloan WT, Quince C, Curtis TP (2018) Temperature, inocula and substrate: Contrasting electroactive consortia, diversity and performance in microbial fuel cells. Bioelectrochemistry 119:43–50. https://doi.org/10.1016/j.bioelechem.2017.07.006
22. Kim H, Kim B, Kim J, Yu J (2015) Effect of organic loading rates and influent sources on energy production in multi-baffled single chamber microbial fuel cell. Desalin Water Treat 56(5):1217–1222. https://doi.org/10.1080/19443994.2014.950986
23. Raghavulu SV, Mohan SV, Goud RK, Sarma PN (2009) Effect of anodic pH microenvironment on microbial fuel cell (MFC) performance in concurrence with aerated and ferricyanide catholytes. Electrochem Commun 11(2):371–375. https://doi.org/10.1016/j.elecom.2008.11.038
24. He Z, Huang Y, Manohar AK, Mansfeld F (2008) Effect of electrolyte pH on the rate of the anodic and cathodic reactions in an air-cathode microbial fuel cell. Bioelectrochemistry 74(1):78–82. https://doi.org/10.1016/j.bioelechem.2008.07.007
25. Vologni V, Kakarla R, Angelidaki I, Min B (2013) Increased power generation from primary sludge by a submersible microbial fuel cell and optimum operational conditions. Bioprocess Biosyst Eng 36(5):635–642. https://doi.org/10.1007/s00449-013-0918-2
26. Radeef AY, Ismail ZZ (2019) Polarization model of microbial fuel cell for treatment of actual potato chips processing wastewater associated with power generation. J Electroanal Chem 836:176–181. https://doi.org/10.1016/j.jelechem.2019.02.001
27. Hernández-Flores G, Poggi-Varaldo HM, Solorza-Feria O, Ponce Noyola MT, Romero-Castañón T, Rinderknecht-Seijas N (2015) Tafel equation based model for the performance of a microbial fuel cell. Int J Hydrogen Energy 40(48):17421–17432. https://doi.org/10.1016/j.ijhydene.2015.06.119
28. Kadivarian M, Dadkhah AA, Esfahany MN (2019) Effect of cell structure and heat pretreating of the microorganisms on performance of a microbial fuel cell. Water Sci Technol. https://doi.org/10.2166/wst.2019.174
29. Wang W, Wei X, Choi D, Lu X, Yang G, Sun C (2015) Chapter 1—Electrochemical cells for medium- and large-scale energy storage: fundamentals. In: Menictas C, Skyllas-Kazacos M, Lim TM (eds) Advances in batteries for medium and large-scale energy storage. Woodhead Publishing, UK, pp 3–28. doi:10.1016/B978-1-78242-013-2.00001-7.

30. Pandey P, Shinde VN, Deopurkar RL, Kale SP, Patil SA, Pant D (2016) Recent advances in the use of different substrates in microbial fuel cells toward wastewater treatment and simultaneous energy recovery. Appl Energy 168:706–723. https://doi.org/10.1016/j.apenergy.2016.01.056
31. Pant D, Van Bogaert G, Diels L, Vanbroekhoven K (2010) A review of the substrates used in microbial fuel cells (MFCs) for sustainable energy production. Bioresour Technol 101(6):1533–1543. https://doi.org/10.1016/j.biortech.2009.10.017
32. Yaws CL (2009) Chapter 12—Diffusion coefficient in water—organic compounds. In: Transport properties of chemicals and hydrocarbons. William Andrew Publishing, Boston, pp 502–593. doi:10.1016/B978-0-8155-2039-9.50017-X.
33. Biffinger JC, Pietron J, Bretschger O, Nadeau LJ, Johnson GR, Williams CC, Nealson KH, Ringeisen BR (2008) The influence of acidity on microbial fuel cells containing Shewanella oneidensis. Biosens Bioelectron 24(4):900–905. https://doi.org/10.1016/j.bios.2008.07.034
34. Rahimnejad M, Ghoreyshi AA, Najafpour G, Jafary T (2011) Power generation from organic substrate in batch and continuous flow microbial fuel cell operations. Appl Energy 88(11):3999–4004. https://doi.org/10.1016/j.apenergy.2011.04.017
35. Jayashree C, Tamilarasan K, Rajkumar M, Arulazhagan P, Yogalakshmi KN, Srikanth M, Banu JR (2016) Treatment of seafood processing wastewater using upflow microbial fuel cell for power generation and identification of bacterial community in anodic biofilm. J Environ Manag 180:351–358. https://doi.org/10.1016/j.jenvman.2016.05.050
36. Sonawane JM, Marsili E, Chandra Ghosh P (2014) Treatment of domestic and distillery wastewater in high surface microbial fuel cells. Int J Hydrogen Energy 39(36):21819–21827. https://doi.org/10.1016/j.ijhydene.2014.07.085
37. Hassan SHA, Kim YS, Oh S-E (2012) Power generation from cellulose using mixed and pure cultures of cellulose-degrading bacteria in a microbial fuel cell. Enzyme Microb Technol 51(5):269–273. https://doi.org/10.1016/j.enzmictec.2012.07.008
38. Jafary T, Rahimnejad M, Ghoreyshi AA, Najafpour G, Hghparast F, Daud WRW (2013) Assessment of bioelectricity production in microbial fuel cells through series and parallel connections. Energy Convers Manage 75(Suppl C):256–262. https://doi.org/10.1016/j.enconman.2013.06.032
39. Haavisto JM, Kokko ME, Lay C-H, Puhakka JA (2017) Effect of hydraulic retention time on continuous electricity production from xylose in up-flow microbial fuel cell. Int J Hydrogen Energy 42(45):27494–27501. https://doi.org/10.1016/j.ijhydene.2017.05.068
40. Santoro C, Rojas-Carbonell S, Awais R, Gokhale R, Kodali M, Serov A, Artyushkova K, Atanassov P (2018) Influence of platinum group metal-free catalyst synthesis on microbial fuel cell performance. J Power Sources 375:11–20. https://doi.org/10.1016/j.jpowsour.2017.11.039
41. Nimje VR, Chen C-Y, Chen C-C, Chen H-R, Tseng M-J, Jean J-S, Chang Y-F (2011) Glycerol degradation in single-chamber microbial fuel cells. Bioresour Technol 102(3):2629–2634. https://doi.org/10.1016/j.biortech.2010.10.062
42. Kim JR, Jung SH, Regan JM, Logan BE (2007) Electricity generation and microbial community analysis of alcohol powered microbial fuel cells. Bioresour Technol 98(13):2568–2577. https://doi.org/10.1016/j.biortech.2006.09.036
43. Zhuang L, Zhou S, Li Y, Yuan Y (2010) Enhanced performance of air-cathode two-chamber microbial fuel cells with high-pH anode and low-pH cathode. Bioresour Technol 101(10):3514–3519. https://doi.org/10.1016/j.biortech.2009.12.105
44. Feng Y, Yang Q, Wang X, Liu Y, Lee H, Ren N (2011) Treatment of biodiesel production wastes with simultaneous electricity generation using a single-chamber microbial fuel cell. Bioresour Technol 102(1):411–415. https://doi.org/10.1016/j.biortech.2010.05.059
45. Yu N, Xing D, Li W, Yang Y, Li Z, Li Y, Ren N (2017) Electricity and methane production from soybean edible oil refinery wastewater using microbial electrochemical systems. Int J Hydrogen Energy 42(1):96–102. https://doi.org/10.1016/j.ijhydene.2016.11.116
46. Santoro C, Ieropoulos I, Greenman J, Cristiani P, Vadas T, Mackay A, Li B (2013) Power generation and contaminant removal in single chamber microbial fuel cells (SCMFCs) treating human urine. Int J Hydrogen Energy 38(26):11543–11551. https://doi.org/10.1016/j.ijhydene.2013.02.070
47. Puig S, Serra M, Coma M, Cabré M, Balaguer MD, Colprim J (2010) Effect of pH on nutrient dynamics and electricity production using microbial fuel cells. Bioresour Technol 101(24):9594–9599. https://doi.org/10.1016/j.biortech.2010.07.082
48. Venkata Mohan S, Mohanakrishna G, Velvizhi G, Babu VL, Sarma PN (2010) Bio-catalyzed electrochemical treatment of real field dairy wastewater with simultaneous power generation. Biochem Eng J 51(1):32–39. https://doi.org/10.1016/j.bej.2010.04.012
49. Divya Priya A, Pydi Setty Y (2019) Cashew apple juice as substrate for microbial fuel cell. Fuel 246:75–78. https://doi.org/10.1016/j.fuel.2019.02.100
50. Gurung A, Oh SE (2015) Rice Straw as a Potential Biomass for Generation of Bioelectrical Energy Using Microbial Fuel Cells (MFCs). Energy Sources, Part A Recover Utilization Environ Effects 37(24):2625–2631. https://doi.org/10.1080/15567036.2012.728678
51. Huang L, Yang X, Quan X, Chen J, Yang F (2010) A microbial fuel cell–electro-oxidation system for coking wastewater treatment and bioelectricity generation. J Chem Technol Biotechnol 85(5):621–627. https://doi.org/10.1002/jctb.2320
52. Tremouli A, Martinos M, Lyberatos G (2017) The effects of salinity, pH and temperature on the performance of a microbial fuel cell. Waste Biomass Valorization 8(6):2037–2043. https://doi.org/10.1007/s12649-016-9712-0
53. Cheng S, Xing D, Logan BE (2011) Electricity generation of single-chamber microbial fuel cells at low temperatures. Biosens Bioelectron 26(5):1913–1917. https://doi.org/10.1016/j.bios.2010.05.016